A New Pulse Active Width Modulation for Multilevel Converters

Concettina Buccella, *Senior Member, IEEE*, Maria Gabriella Cimoroni, Mario Tinari, and Carlo Cecati, *Fellow, IEEE*

***Abstract*—This paper proposes a new pulse amplitude width modulation (PAWM) procedure for cascaded H-bridge multilevel inverters fed by dc voltage sources with unequal amplitudes. With proposed procedure, the generated output voltage is obtained modulating a sinusoidal reference signal at the desired fundamental frequency with equally spaced switching angles. It has been analytically demonstrated that, under these assumptions, all harmonics except those of order $n = 2kl \pm 1$, $k = 1, 2, \ldots$ are deleted from the output voltage waveform. After a detailed description of the method and a comparative analysis with others existing in the literature, its harmonics elimination capability has been experimentally verified with 5-, 7-, 9-, and 11-level cascaded H-bridge inverters, moreover, it has been mathematically demonstrated that it reduces total harmonic distortion below 5% with a 17-level inverter and it is capable of eliminating the first 49 harmonics considered by standards with a 27-level inverter.**

***Index Terms*—Multilevel inverters, pulse active width modulation (PAWM), selective harmonics elimination (SHE), selective harmonics mitigation (SHM), total harmonic distortion (THD).**

I. Introduction

BECAUSE of their topology, cascaded H-bridge (CHB) multilevel converters can successfully operate with fundamental or low frequency as well as with pulsewidth modulation, offering significantly better output waveforms, medium voltage capabilities, and often better efficiency than conventional two-level converters. Selective harmonic elimination (SHE) modulation methods are quite popular in high power multilevel converters because while eliminating predefined low-order harmonics, they are capable to maintain the fundamental voltage at the desired level [1], [2]. SHE methods can be classified in SHE-pulsewidth modulation (SHE-PWM), e.g., [1]–[3] and SHE-pulse-amplitude modulation (SHE-PAM) [4], [5]. Consid-

Manuscript received December 22, 2017; revised March 22, 2018, May 11, 2018, July 26, 2018, and September 30, 2018; accepted October 12, 2018. Date of publication October 30, 2018; date of current version May 22, 2019. This project was supported in part by DigiPower srl, L'Aquila, Italy, under Grant "HORIZON 2020" PON I&C2014–2020 and in part by Progetto "Comodes" under Grant F/050220/X32 CUP B18I15000100008. Recommended for publication by Associate Editor G. Konstantinou. *(Corresponding author: Concettina Buccella.)*

The authors are with the Department of Information Engineering, Computer Science and Mathematics, University of L'Aquila, L'Aquila 67100, Italy, and also with DigiPower srl, L'Aquila 67100, Italy (e-mail:

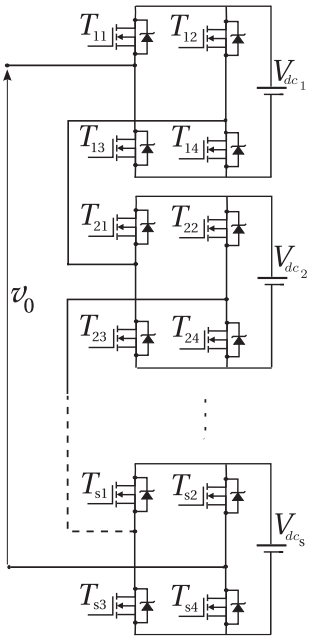

Fig. 1. Multilevel inverter configuration.

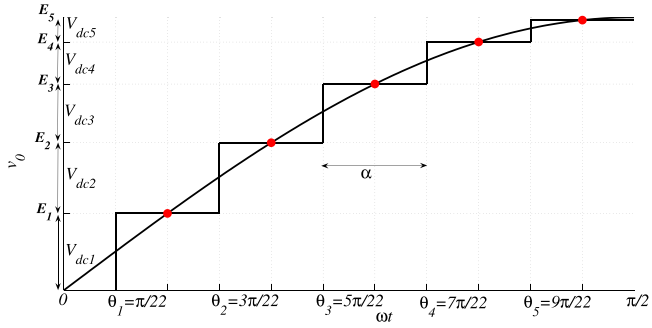

Fig. 2. 11-level inverter output voltage waveform.

a recursive algorithm has been used to solve each triangular equation. Fast and accurate analytical methods have been presented in [17] and [18], for a 5-level inverter. It is worth noticing that none of these methods provides switching states for continuously varying operating point applications. This paper presents a pulse active width modulation (PAWM) characterized by equally spaced switching angles. It has been developed for l-level CHB inverters fed by s unequal dc voltage sources. Adopting the proposed method, all harmonics, except those of order $n = 2kl \pm 1, k = 1, 2, \ldots$ disappear from the output voltage. Its modulation index is bounded within the range $0 \leq m \leq 1$, where closed solutions always exist. A mathematical proof of the number and the order of deleted harmonics is given and some experimental results have been included for validation purposes. It is worth noticing that with the proposed method, neither switching angles nor output voltage total harmonic distortion (THD) depend on the modulation index m, which can be easily modified by changing dc voltage levels. The proposed method can be successfully adopted in all those applications adopting variable dc sources, such as photovoltaic energy systems, uninterruptible power supplies (UPS), electric vehicle powertrains, etc. The advantages and feasibility of the proposed PAWM have been evaluated through comparative analysis with the methods described in [4], [5], [13], [14], and [17]–[20].

II. Pulse Active Width Modulation

An l-level cascaded inverter, consisting of s H-bridge fed by s unequal dc voltage sources $V_{\mathrm{dc}1}, V_{\mathrm{dc}2}, \ldots, V_{\mathrm{dc}s}$, has been considered, as shown in Fig. 1. The following hypotheses are assumed.

1) The output voltage waveform v_0 is modulated by a reference sinusoidal signal (RSS) at fundamental frequency.
2) The switching angles are chosen as $\theta_k = (2k-1)\frac{\pi}{2l}, k = 1, 2 \ldots, s$ and are equispaced with step $\alpha = \frac{\pi}{l}, l = 2s+1$ within the interval $[0, \pi/2]$.
3) The output v_0, consists of s levels $E_1, E_2, \ldots E_s$ calculated in the following manner: considering a generic interval $[\theta_k, \theta_{k+1}]$, the level E_k is fixed at the magnitude of the RSS in the middle point, given by

$$E_k = V_m \sin\left(\frac{\theta_k + \theta_{k+1}}{2}\right) = V_m \sin(k\alpha) \;\; k = 1, 2, \ldots, s \tag{1}$$

where V_m is the peak value of the RSS (see Fig. 2).

The amplitudes of the dc voltage sources are as follows:

$$V_{\mathrm{dc}k} = E_k - E_{k-1} \qquad k = 1, 2, \ldots, s \tag{2}$$

with $E_0 = 0$ and $\theta_{s+1} = \pi/2$.

Under these assumptions and applying the Fourier series expansion, the amplitude of the nth harmonic V_n of v_0 is given by

$$V_n = \frac{4}{n\pi} \sum_{k=1}^{s} (E_k - E_{k-1}) \cos(n\theta_k). \tag{3}$$

Because v_0 is an odd function, even harmonics are absent and (3) holds only for odd harmonics.

Just to exemplify, an 11-level inverter is considered in Fig. 2. In this case, $s = 5$, $l = 11$, $\theta_1 = \pi/22$, $\theta_2 = 3\pi/22$, $\theta_3 = 5\pi/22$, $\theta_4 = 7\pi/22$, and $\theta_5 = 9\pi/22$. The amplitude of the first harmonic must be set equal to the modulation index value.

Rearranging (3), we obtain:

$$V_n = \frac{4}{n\pi} \sum_{k=1}^{s} E_k \left[\cos\left(n(2k-1)\frac{\alpha}{2}\right) - \cos\left(n(2k+1)\frac{\alpha}{2}\right)\right]. \tag{4}$$

The term $\cos((2s+1)n\frac{\alpha}{2}) = 0$ because when n is odd then $(2s+1)n\alpha/2 = n\pi/2$.

Applying the Prosthaphaeresis formula in (4) and substituting E_i with (1), we obtain

$$V_n = \frac{4 \cdot 2V_m}{n\pi} \sin\left(n\frac{\alpha}{2}\right) \left[\sum_{k=1}^{s} \sin(nk\alpha) \sin(k\alpha)\right]. \tag{5}$$

After some goniometric manipulations, we obtain

$$V_n = \frac{4 \cdot V_m}{n\pi} \sin\left(n\frac{\alpha}{2}\right) \sum_{k=1}^{s} [\cos((n-1)k\alpha) - \cos((n+1)k\alpha)]. \quad (6)$$

III. Analytical Computation of the n Values Giving $V_n = 0$ for a Variable l

This section aims at demonstrating that the proposed modulation technique eliminates all harmonics, except those of order $n = 2kl \pm 1$, $k = 1, 2, \ldots$. The case $n = -1$ is not significant for the considered applications. Notice that in (6), the term $\sin(n\frac{\alpha}{2})$ is equal to zero only if the term $n = 2kl$ is even, hence, only the sum $\sum_{k=1}^{s}[\cos((n-1)k\alpha) - \cos((n+1)k\alpha)]$ contributes to the computation of n giving $V_n = 0$ [21].

Theorem 1: The sum

$$\sum_{k=1}^{s} [\cos((n-1)k\alpha) - \cos((n+1)k\alpha)] \quad (7)$$

$\alpha = \frac{\pi}{l}$, $l = 2s+1$, $s = 2, 3, \ldots$ is equal to zero for all odd n, $n \neq 2kl \pm 1$, $k = 0, 1, 2, \ldots$.

Proof: Introducing the function $S_l(h)$

$$S_l(h) = \sum_{k=1}^{s} \cos(hk\alpha) \quad (8)$$

with $h = n \pm 1$ and applying Eulero's formula to (8), the following expression is obtained:

$$S_l(h) = \frac{1}{2}\left[\sum_{k=1}^{s}\left(e^{ih\alpha}\right)^k + \sum_{k=1}^{s}\left(e^{-ih\alpha}\right)^k\right] \quad (9)$$

with i imaginary unit. Since the sums in (9) are geometrical, (10) is obtained as

$$S_l(h) = \frac{1}{2}\left[e^{ih\alpha}\frac{1-e^{ih\alpha s}}{1-e^{ih\alpha}} + e^{-ih\alpha}\frac{1-e^{-ih\alpha s}}{1-e^{-ih\alpha}}\right] \quad (10)$$

$h \neq 2kl$, $k = 0, 1, 2, \ldots$.

After some mathematical manipulations (see the Appendix), we obtain

$$S_l(h) = \frac{\sin\left(h\frac{\pi}{4}\frac{l-1}{l}\right)}{\sin\left(h\frac{\pi}{2l}\right)} \cos\left(h\frac{\pi}{4}\frac{l+1}{l}\right) \quad (11)$$

with $h \neq 2lk$, $k = 0, 1, 2, \ldots$. Rearranging (11) by using goniometric formulas, the following relationship can be obtained:

$$S_l(h) = \frac{1}{2}\left[\frac{\sin\left(h\frac{\pi}{2}\right)}{\sin\left(h\frac{\pi}{2l}\right)} - 1\right]. \quad (12)$$

From (8) and (12), the sum (7) becomes

$$\sum_{k=1}^{s} [\cos((n-1)k\alpha) - \cos((n+1)k\alpha)] = S_l(n-1) - S_l(n+1) = \frac{1}{2}\left[\frac{\sin\left((n-1)\frac{\pi}{2}\right)}{\sin\left((n-1)\frac{\pi}{2l}\right)} - \frac{\sin\left((n+1)\frac{\pi}{2}\right)}{\sin\left((n+1)\frac{\pi}{2l}\right)}\right] \quad (13)$$

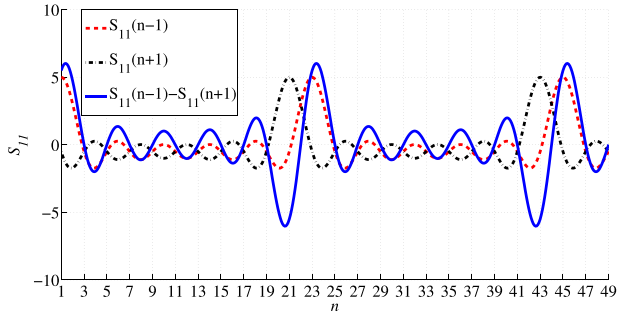

Fig. 3. Behavior of the functions $S_{11}(n-1)$, $S_{11}(n+1)$ and their difference.

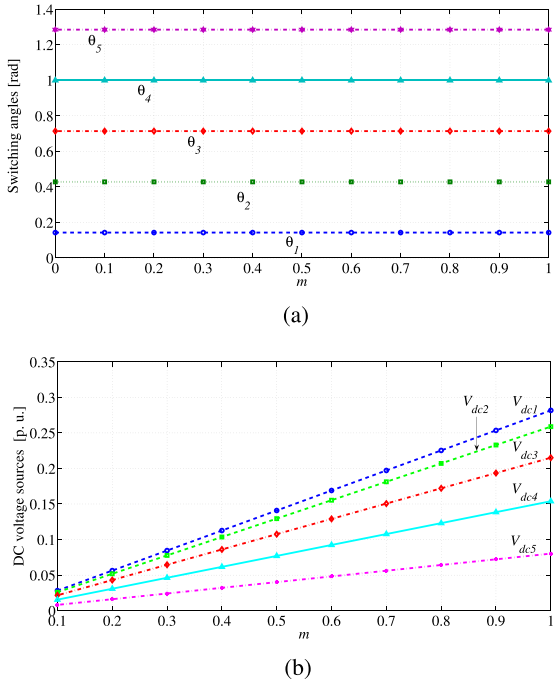

Fig. 4. Variations in 11-level CHB inverter. (a) Switching angles. (b) DC voltage sources with m.

and, after easy mathematical manipulations, the following relationship can be obtained:

$$\sum_{k=1}^{s} [\cos((n-1)k\alpha) - \cos((n+1)k\alpha)] = -\cos\left(n\frac{\pi}{2}\right)\frac{\cos\left(\frac{\pi}{2l}\right)\sin\left(n\frac{\pi}{2l}\right)}{\sin\left((n-1)\frac{\pi}{2l}\right)\sin\left((n+1)\frac{\pi}{2l}\right)}. \quad (14)$$

For n odd, $n \neq 2lk \pm 1$, $k = 0, 1, 2, \ldots$, (14) is zero.

In order to evaluate (14) in $n = 2lk \pm 1$, where it is not defined (because has the form $0/0$), the application of the De L'Hospital rule leads to

$$\lim_{n \to 2lk \pm 1}\left[-\cos\left(\frac{\pi}{2l}\right)\cos\left(n\frac{\pi}{2}\right) \times \frac{\sin\left(n\frac{\pi}{2l}\right)}{\sin\left((n-1)\frac{\pi}{2l}\right)\sin\left((n+1)\frac{\pi}{2l}\right)}\right] = \pm\frac{l}{2}. \quad (15)$$

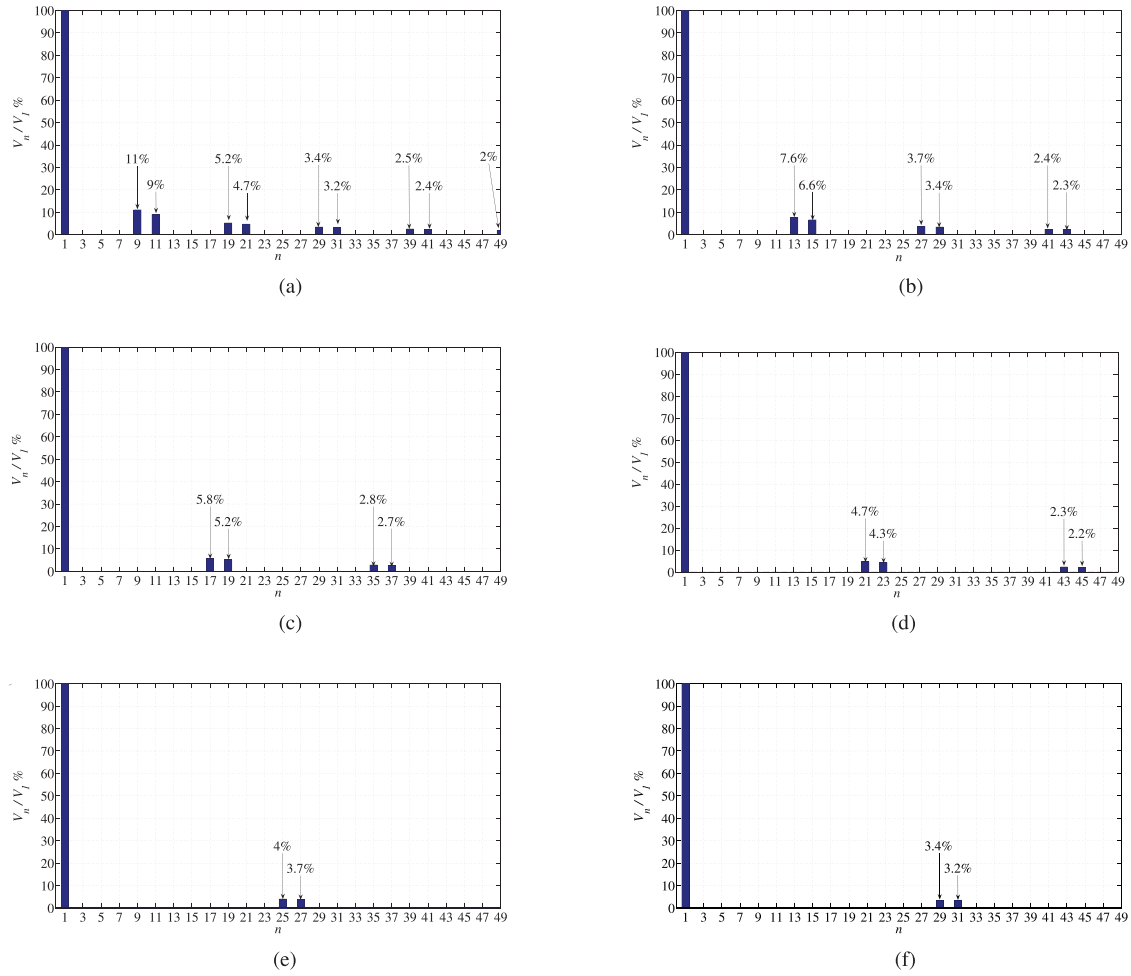

Fig. 5. Harmonic analysis in an l-level CHB inverter. (a) $l = 5$. (b) $l = 7$. (c) $l = 9$. (d) $l = 11$. (e) $l = 13$. (f) $l = 15$.

Therefore, it is demonstrated that for $n = 2lk \pm 1$, the sum $\sum_{k=1}^{s}[\cos((n-1)k\alpha) - \cos((n+1)k\alpha)] \neq 0$. From (14) and (15), the thesis is demonstrated. ■

Just to include an example, an 11-level inverter is considered here. Fig. 3 shows the functions $S_{11}(n-1)$, $S_{11}(n+1)$ and their difference, highlighting that only the harmonics with order $n = 21, 23, 43, 45$ are not zero. Fig. 4 shows the effect of the modulation index m on the switching angles and on the dc voltage sources. It can be observed that the switching angles remain constant, whereas the dc voltage varies linearly with m.

Fig. 5 shows the harmonic analysis obtained for l-level CHB inverters with $l = 5, 7, 9, 11, 13, 15$.

IV. Comparison With Other Modulation Techniques

In order to demonstrate the quality of PAWM, it has been compared with some methods already proposed in the literature.

A. Comparison With the Method Described in [5]

The method proposed in [5] has been implemented and compared with PAWM. It has been found that the proposed method cancels more harmonics than the one proposed in [5] but it does not delete the harmonics having order

$$2lk \pm 1 \qquad k = 1, 2, \ldots. \tag{16}$$

On the other side, the procedure in [5] does not delete the harmonics having order

$$2Lk \pm 1 \; k = 1, 2, \ldots \tag{17}$$

where $L = l - 1$, therefore

$$2\,(l-1)\,k \pm 1 = 2lk \pm 1 - 2k \quad k = 1, 2, \ldots. \tag{18}$$

Comparing (16) with (18), the term $2k$ implies that in [5], the first not deleted harmonic (for $k = 1$) has order $(2l - 3)$, which is lower than the order $(2l - 1)$ obtained by PAWM. For example, for a 5-level inverter and considering up to the 49th harmonic, PAWM does not cancel 9 harmonics, but the procedure in [5] does not delete 12 harmonics (see Table I).

It can be noted that in PAWM, the first switching angle is always different by zero: in fact, the switching angles are chosen, such as $\theta_k = (2k-1)\pi/2l$, $k = 1, 2 \ldots, s$. In [5], the first angle is always equal to zero: in fact, the angles are chosen, such as $\theta_k = (k-1)\pi/(l-1)$, $k = 1, 2, \ldots, s$ (see [5, formula (5)]). Table I summarizes, for multilevel inverters with $l = 5, 7, 9, 11, 13$ and considering up to 49th harmonic, the

TABLE I
COMPARISON BETWEEN PAWM AND THE TECHNIQUE IN [5]

		l = 5		7		9		11		13	
		PAWM	[5]	PAWM	[5]	PAWM	[5]	PAWM	[5]	PAWM	[5]
n	3	x	x	x	x	x	x	x	x	x	x
	5	x	x	x	x	x	x	x	x	x	x
	7	x	●	x	x	x	x	x	x	x	x
	9	●	●	x	x	x	x	x	x	x	x
	11	●	x	x	●	x	x	x	x	x	x
	13	x	x	●	●	x	x	x	x	x	x
	15	x	●	●	x	x	●	x	x	x	x
	17	x	●	x	x	●	●	x	x	x	x
	19	●	x	x	x	●	x	x	●	x	x
	21	●	x	x	x	x	x	●	●	x	x
	23	x	●	x	●	x	x	●	x	x	●
	25	x	●	x	●	x	x	x	x	●	●
	27	x	x	●	x	x	x	x	x	●	x
	29	●	x	●	x	x	x	x	x	x	x
	31	●	●	x	x	x	●	x	x	x	x
	33	x	●	x	x	x	●	x	x	x	x
	35	x	x	x	●	●	x	x	x	x	x
	37	x	x	x	●	●	x	x	x	x	x
	39	●	●	x	x	x	x	x	●	x	x
	41	●	●	●	x	x	x	x	●	x	x
	43	x	x	●	x	x	x	●	x	x	x
	45	x	x	x	x	x	x	●	x	x	x
	47	x	●	x	x	x	●	x	x	x	●
	49	●	●	x	●	x	●	x	x	x	●

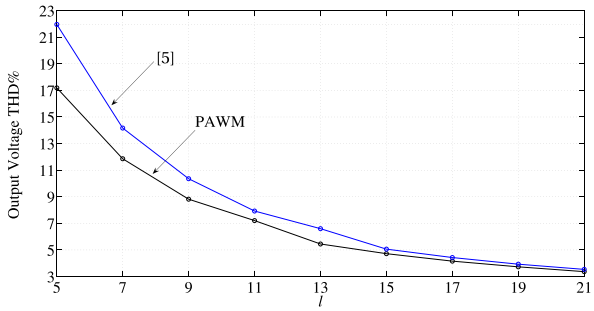

Fig. 6. Comparison between output voltage THDs% at different number of levels.

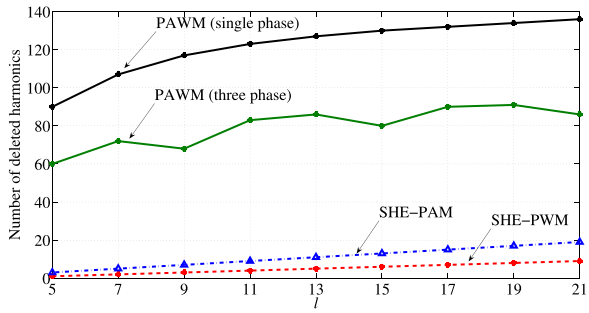

Fig. 7. Number of deleted harmonics as function of number of levels.

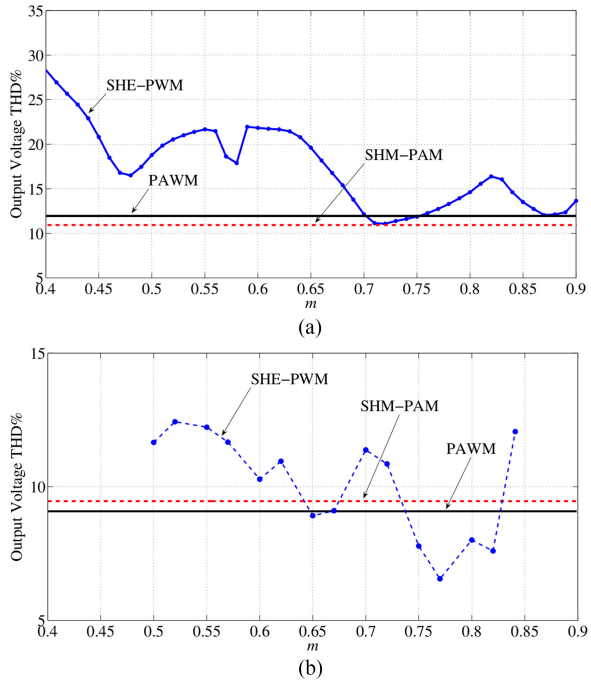

Fig. 8. Output voltage THD% obtained with PAWM, SHE-PWM and SHM-PAM. (a) 5-level inverter. (b) 7-level inverter.

harmonics deleted by PAWM and by the technique in [5]. The red dots represent the not-canceled harmonics with PAWM, the blue dots represent the not-canceled harmonics with modulation in [5], and the "x" symbols represent the deleted ones.

The THD% of the output voltage is defined as:

$$\text{THD\%} = \frac{\sqrt{\sum_{i=3,5\ldots}^{49} V_i^2}}{V_1} 100 \tag{19}$$

and it is constant, whereas the modulation index varies. Fig. 6 shows the output voltage THD% for the considered modulations applied to an inverter with the number of levels up to $l = 21$. The better performance of PAWM over [5] is evident.

B. Comparison of PAWM With Conventional SHE-SHM-PWM and SHE-SHM-PAM Methods

In this section, the performance of the proposed PAWM has been compared with those of some implementations of conventional SHE-SHM-PWM: [17], [18], [19], [20], and of SHE-SHM-PAM: [4], [13], [14]. One switching transition has been considered per each level, which leads to the identical switching frequency in SHE-SHM methods. Conventional SHE-PWM and SHE-PAM eliminate a total number of $l - 3/2$ and $l - 2$ harmonics, respectively. Fig. 7 shows, for the proposed PAWM and for the considered conventional SHE-PWM and SHE-PAM, the number of deleted harmonics as a function of the number of levels. The analysis has been carried out considering up to the 301th harmonic. PAWM eliminates a larger number of harmonics than conventional SHE methods. For example, considering a single-phase, 13-level CHB inverter, the total number of harmonics eliminated by SHE-PWM, SHE-PAM, and PAWM are 5, 11, 127, respectively, whereas considering a three-phase inverter, the total number of harmonics eliminated are 5, 11, 86, respectively.

In the following, three-phase systems have been considered. Since the third and multiple harmonics are intrinsically eliminated, they should not be controlled. The output voltage THD% in 5- and 7-level three-phase inverters have been computed and the results are shown in Fig. 8(a) and (b), respectively. Simulations have been carried out using PAWM and SHM-PAM in [13] and [14] to mitigate harmonics with order $k = 5, 7, \ldots, 49$

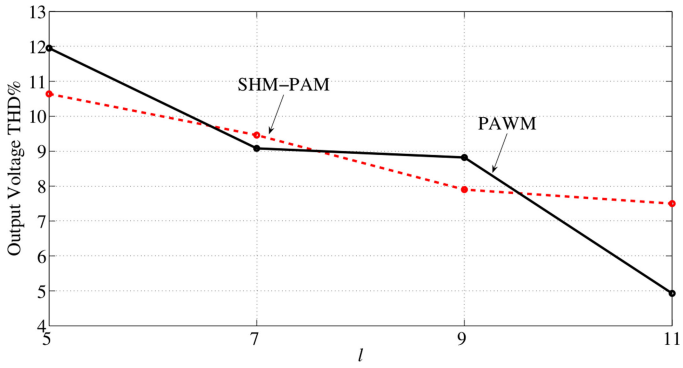

Fig. 9. Output voltage THD% at different levels with PAWM and SHM-PAM.

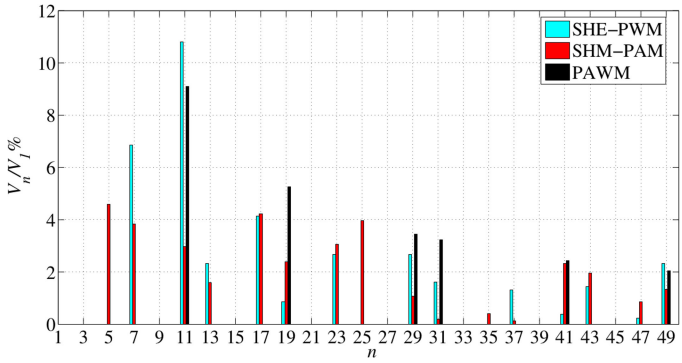

Fig. 10. Weighted THD of a three-phase 5-level CHB inverter with PAWM, SHE-PWM, and SHM-PAM.

and SHE-PWM in [17]–[20] to eliminate the fifth harmonic in 5-level inverters, and the fifth and the seventh harmonics in 7-level inverters. Regarding SHE-PWM, if for an assigned m, multiple solutions exist, then the graph in Fig. 8(a) refers to the values returning the lower THD. It has been found that, for a 7-level inverter, the SHE-PWM solution exists only if $m = [0.5, 0.84]$. Fig. 9 shows that, due to the intrinsic elimination of the third and multiple harmonics in three-phase systems, adopting 5- and 9-level inverters, proposed PAWM gives a little bit higher THD% than SHM-PAM, but PAWM outperforms SHM-PAM with 7- and 11-level inverters. The weighted THD (WTHD), i.e., the harmonics amplitudes weighted with respect to the fundamental ($\frac{V_n}{V_1}\%$) shown in Fig. 10 is computed for a three phase CHB 5-level inverter modulated by PAWM, by SHE-PWM for the fifth harmonic elimination and considering $m = 0.8$ [17] and by SHM-PAM used to mitigate the harmonics of order $k = 5, 7, \ldots, 49$ [13], [14].

V. Experimental Results

Experimental results have been obtained using 5-, 7-, 9- and 11-level single-phase inverters realized cascading H-bridge cells produced by DigiPower srl and rated 600 V, 40 A each [22]. Fig. 11 shows the 9-level inverter configuration. Each cell can operate at switching frequency exceeding 40 kHz and has its own DSP that provides to data acquisition, signal conditioning, and calculations, moreover, it includes serial peripheral communication (SPI) channels. The whole multilevel converter is controlled by a field programmable gate array (FPGA) Intel

Fig. 11. Experimental setup.

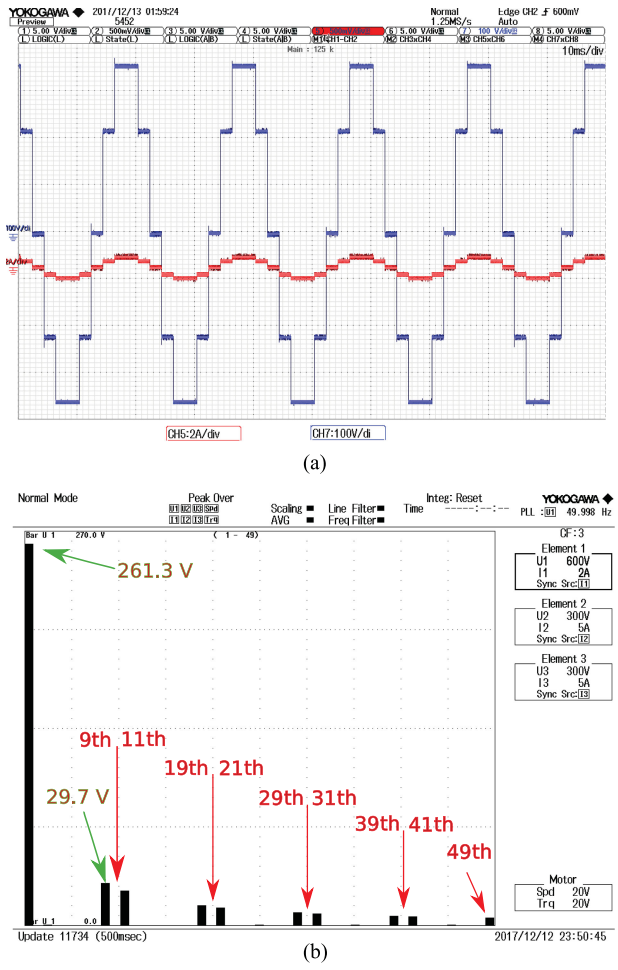

Fig. 12. Experimental results in a 5-level inverter. (a) Output voltage (blue line) and current (red line) waveforms. (b) Harmonics amplitudes of output voltage in volt.

CycloneV model SE 5CSEBA6U23I7, programed using Quartus [23], [24]. In this application, the FPGA is in charge of pulse generation with 32-b resolution and implements interlock logic with deadband. Modulation patterns are transmitted to the H-bridges through SPI channels. Each H-bridge is supplied according to (2) with $V_m = 380$ V at fundamental frequency 50 Hz using a programmable dc power supply model Lambda—

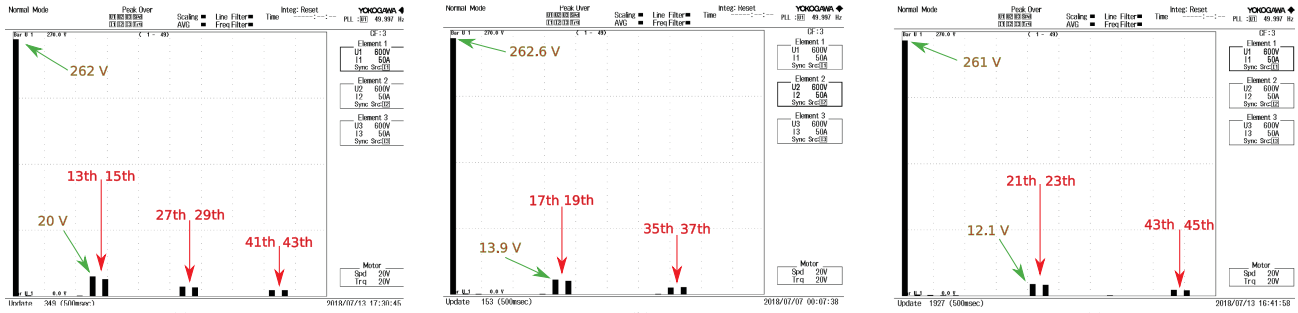

(a) (b) (c)

Fig. 13. Harmonics amplitudes of output voltage. (a) 7-level inverter. (b) 9-level inverter. (c) 11-level inverter.

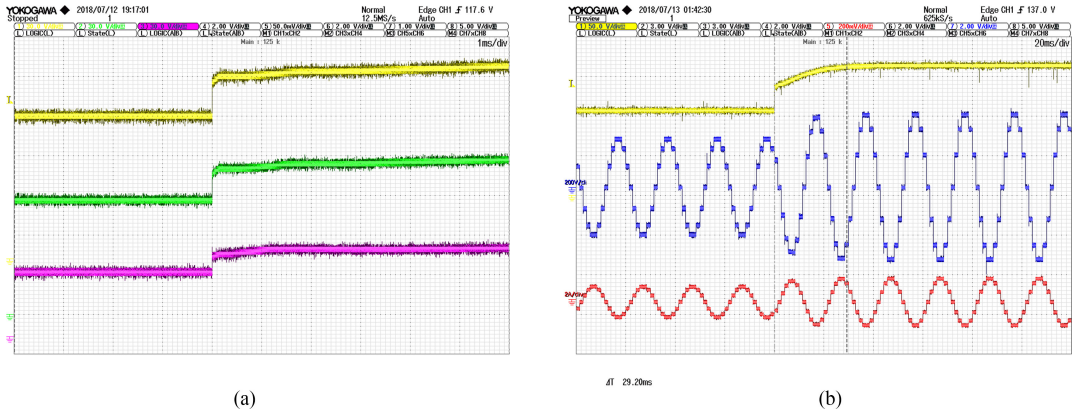

(a) (b)

Fig. 14. Transient response. (a) DC voltage sources step to vary modulation index from $m = 0.64$ to $m = 1$. (b) Output voltage (blue line) and current (red line) waveforms.

TABLE II
OUTPUT VOLTAGE THD% VERSUS DESIGNED DC LINK VOLTAGES DISTURBANCES

	V_{dc1} [V]	V_{dc2} [V]	V_{dc3} [V]	THD%
Designed DC voltages	V_{dc1r}=164.9	V_{dc2r}=132.2	V_{dc3r}=73.38	11.86
Case#1	V_{dc1r}-10%=148.4	V_{dc2r}+10%=145.4	V_{dc3r}+5%=77.1	12.32
Case#2	V_{dc1r}-20%=131.9	V_{dc2r}+20%=158.7	V_{dc3r}+10%=80.7	13.51
Case#3	V_{dc1r}-30%=115.4	V_{dc2r}+30%=171.9	V_{dc3r}+20%=88.1	15.46

Genesys 600–2.6, rated 600 V, 2.6 A. The load connected to the output terminals has $R = 315\,\Omega$ and $L = 11.56$ mH.

An eight-channel Digital Oscilloscope Yokogawa DLM4058 (2.5 GS/s 500 MHz) and a three-phase power meter Yokogawa WT1800 complete the experimental setup.

Figs. 12 and 13 show the obtained results, which are in full agreement with the previous theoretical analysis.

The robustness of PAWM to disturbances around the designed dc link voltages is verified considering a 7-level inverter connected with the RL load.

Assuming the designed dc voltages equal to $V_{\mathrm{dc}1r} = 164.9\,\mathrm{V}, V = 132.2\,\mathrm{V}, V_{\mathrm{dc}3r} = 73.38\,\mathrm{V}$, the tests named Case#1, Case#2, and Case#3, during which the considered disturbances are applied, are executed and the corresponding output voltages THD% are measured. Table II summarizes both the applied disturbances and the corresponding THD%. It can be noticed that, during the worst Case#3, THD% increases approximately the same percentage of the dc voltages disturbances, therefore, the system is well conditioned. In the best case, i.e., Case#1, the increase of the THD% is lower than disturbances percentages.

The same 7-level configuration with the same load has been used to evaluate transient conditions during modulation index variations, the latter obtained modifying, for each module, (2), i.e., $V_{\mathrm{dc}k}$, $k = 1, 2, 3$. DC voltages values change from $V_{\mathrm{dc}1} = 108.5\,\mathrm{V}, V_{\mathrm{dc}2} = 87\,\mathrm{V}, V_{\mathrm{dc}3} = 48.3\,\mathrm{V}$ corresponding to $m = 0.657$ to the new values $V_{\mathrm{dc}1} = 164.9\,\mathrm{V}, V_{\mathrm{dc}2} = 132.2\,\mathrm{V}, V_{\mathrm{dc}3} = 73.38\,\mathrm{V}$ corresponding to $m = 1$ [see Fig. 14(a)]. Voltage and current transient responses are shown in Fig. 14(b). It can be noticed that the steady-state condition is reached after about 30 ms.

VI. CONCLUSION

A new procedure based on PAWM has been developed for CHB converters fed by unequal dc voltage sources. The proposed procedure identifies equally spaced switching angles and performs a modulation of the output voltage on the base of an RSS signal fixed at the fundamental frequency. A mathematical proof has been presented demonstrating that PAWM deletes all harmonics embedded within the output voltage waveform of an l-level inverter, except those of order $n = 2kl \pm 1, k = 1, 2, \ldots$.

Harmonic elimination capability of PAWM in single- and three-phase cascaded multilevel inverters has been validated by simulation and experimental results as well as by comparisons with some methods described in the literature. The main features of PAWM can be summarized as follows.

1) High efficiency, obtained due to fundamental switching frequency operations.
2) More harmonics eliminated than using other methods: for a chosen number of levels and for the whole modulation index range $(0 \leq m \leq 1)$ it fixes, in optimal way, both the switching angles as well as the amplitudes of the dc voltages.
3) THD% does not depend on the modulation index.
4) Main grid code requirement fulfilment (THD% $< 5\%$) without any passive filter using a 17-level inverter.
5) Full harmonics elimination (up to 49th order) using a 27-level inverter.

Applications of PAWM are numerous as it can be successfully implemented on multilevel converters with dc/dc converter front-end, among the others: photovoltaic and wind generators and UPS.

APPENDIX

Formula (10) can be written as

$$\begin{aligned} S_l(h) &= \frac{1}{2}\left[e^{ih\alpha}\frac{1-e^{ih\alpha s}}{1-e^{ih\alpha}} + \frac{1}{e^{ih\alpha}}\frac{1-\frac{1}{e^{ih\alpha s}}}{1-\frac{1}{e^{ih\alpha}}}\right] \\ &= \frac{1}{2}\left[e^{ih\alpha}\frac{1-e^{ih\alpha s}}{1-e^{ih\alpha}} + \frac{1}{e^{ih\alpha s}}\frac{1-e^{ih\alpha s}}{1-e^{ih\alpha}}\right] \\ &= \frac{1}{2}\frac{1-e^{ih\alpha s}}{1-e^{ih\alpha}}\left(e^{ih\alpha} + \frac{1}{e^{ih\alpha s}}\right) \\ &= \frac{1}{2}\frac{1-e^{ih\alpha s}}{1-e^{ih\alpha}}\left(\frac{e^{ih\alpha(s+1)}+1}{e^{ih\alpha s}}\right) \\ &= \frac{e^{-ih\alpha\frac{s}{2}}-e^{ih\alpha\frac{s}{2}}}{e^{-ih\frac{\alpha}{2}}-e^{ih\frac{\alpha}{2}}}\frac{e^{ih\alpha\frac{s}{2}}}{e^{ih\frac{\alpha}{2}}}\frac{e^{ih\alpha\frac{s+1}{2}}+e^{-ih\alpha\frac{s+1}{2}}}{2}\frac{e^{ih\alpha\frac{s+1}{2}}}{e^{ih\alpha s}} \\ &= \frac{\sin\left(h\alpha\frac{s}{2}\right)}{\sin\left(h\frac{\alpha}{2}\right)}\cos\left(h\alpha\frac{s+1}{2}\right)\frac{e^{ih\alpha\frac{s+1}{2}}\,e^{ih\alpha\frac{s}{2}}}{e^{ih\alpha s}\,e^{ih\frac{\alpha}{2}}}. \end{aligned}$$

Since $\frac{e^{ih\alpha s+1/2}\,e^{ih\alpha s/2}}{e^{ih\alpha s}\,e^{ih\alpha/2}} = e^{ih\alpha 0} = 1$, the previous equation becomes

$$\frac{\sin\left(h\alpha\frac{s}{2}\right)}{\sin\left(h\frac{\alpha}{2}\right)}\cos\left(h\alpha\frac{s+1}{2}\right) = \frac{\sin\left(h\frac{\pi}{4}\frac{l-1}{l}\right)}{\sin\left(h\frac{\pi}{2l}\right)}\cos\left(h\frac{\pi}{4}\frac{l+1}{l}\right)$$

that is formula (11), which can be written as

$$\frac{\sin\left(h\left(\frac{\pi}{4}-\frac{\pi}{4l}\right)\right)}{\sin\left(h\frac{\pi}{2l}\right)}\cos\left(h\left(\frac{\pi}{4}+\frac{\pi}{4l}\right)\right).$$

By using the goniometric formula $\sin p\cos q = \frac{1}{2}[\sin(q+p) - \sin(q-p)]$, the previous formula becomes

$$\frac{1}{2}\frac{\sin\left(h\frac{\pi}{2}\right)-\sin\left(h\frac{\pi}{2l}\right)}{\sin\left(h\frac{\pi}{2l}\right)} = \frac{1}{2}\left[\frac{\sin\left(h\frac{\pi}{2}\right)}{\sin\left(h\frac{\pi}{2l}\right)} - 1\right]$$

that is formula (12). By substituting $(n-1)$ and $(n+1)$ to h, formula (13) is obtained

$$\begin{aligned} &\sum_{k=1}^{s}\left[\cos\left((n-1)\,k\alpha\right) - \cos\left((n+1)\,k\alpha\right)\right] \\ &\quad = S_l\,(n-1) - S_l\,(n+1) \\ &\quad = \frac{1}{2}\left[\frac{\sin\left((n-1)\,\frac{\pi}{2}\right)}{\sin\left((n-1)\,\frac{\pi}{2l}\right)} - \frac{\sin\left((n+1)\,\frac{\pi}{2}\right)}{\sin\left((n+1)\,\frac{\pi}{2l}\right)}\right]. \end{aligned}$$

Considering S as a function in the variable n, by applying to the numerators, the goniometric formula $\sin(q \pm p) = \sin p\cos q \pm \sin q\cos p$, the previous formula becomes

$$\begin{aligned} &-\frac{1}{2}\cos n\frac{\pi}{2}\left[\frac{1}{\sin\left((n-1)\,\frac{\pi}{2l}\right)} + \frac{1}{\sin\left((n+1)\,\frac{\pi}{2l}\right)}\right] \\ &\quad = -\frac{1}{2}\cos n\frac{\pi}{2}\,\frac{\sin\left((n+1)\,\frac{\pi}{2l}\right)+\sin\left((n-1)\,\frac{\pi}{2l}\right)}{\sin\left((n-1)\,\frac{\pi}{2l}\right)\,\sin\left((n+1)\,\frac{\pi}{2l}\right)} \\ &\quad = -\cos n\frac{\pi}{2}\,\frac{\sin\left(n\frac{\pi}{2l}\right)\cos\left(\frac{\pi}{2l}\right)}{\sin\left((n-1)\,\frac{\pi}{2l}\right)\,\sin\left((n+1)\,\frac{\pi}{2l}\right)} \end{aligned}$$

that is (14).

REFERENCES

[1] M. S. A. Dahidah, G. Konstantinou, and V. G. Agelidis, "A review of multilevel selective harmonic elimination PWM: Formulations, solving algorithms, implementation and applications," *IEEE Trans. Power Electron.,* vol. 30, no. 8, pp. 4091–4106, Aug. 2015.

[2] H. Zhao, T. Jin, S. Wang, and L. Sun, "A real-time selective harmonic elimination based on a transient-free inner closed-loop control for cascaded multilevel inverters," *IEEE Trans. Power Electron.*, vol. 31, no. 2, pp. 1000–1014, Feb. 2016.

[3] R. P. Aguilera *et al.*, "Selective harmonic elimination model predictive control for multilevel power converters,"*IEEE Trans. Power Electron.*, vol. 32, no. 3, pp. 2416–2426, Mar. 2017.

[4] E. Mohammadhossein, G. Negareh, V. D. Mahinda, and L. M. Wynand, "Particle swarm optimisation-based modified SHE method for cascaded H-bridge multilevel inverters," *IET Power Electron.*, vol. 10, no. 1, pp. 18–28, 2017.

[5] P. L. Kamani and M. A. Mulla, "Middle-level SHE pulse-amplitude modulation for cascaded multilevel inverters," *IEEE Trans. Ind. Electron.*, vol. 65, no. 3, pp. 2828–2833, Mar. 2018.

[6] M. Ahmed, A. Sheir, and M. Orabi, "Real-time solution and implementation of selective harmonic elimination of seven-level multilevel inverter," *IEEE J. Emerg. Sel. Topics Power Electron.*, vol. 5, no. 4, pp. 1700–1709, Dec. 2017.

[7] M. Hajizadeh and S. H. Fathi, "Selective harmonic elimination strategy for cascaded H-bridge five-level inverter with arbitrary power sharing among the cells," *IET Power Electron.*, vol. 9, no. 1, pp. 95–101, 2016.

[8] L. M. Tolbert, J. N. Chiasson, Z. Du, and K.J. McKenzie, "Elimination of harmonics in multilevel converter with nonequal DC sources," *IEEE Trans. Ind. Appl.*, vol. 41, no. 1, pp. 75–82, Jan./Feb. 2005.

[9] H. Taghizadeh and M. T. Hagh, "Harmonic elimination of cascade multilevel inverters with nonequal DC sources using particle swarm optimization," *IEEE Trans. Power Electron.*, vol. 57, no. 11, pp. 3678–3684, Nov. 2010.

[10] M. G. H. Aghdam, S. H. Fathi, and G. B. Gharehpetian, "Elimination of harmonics in a multi-level inverter with unequal DC sources using the homotopy algorithm," in *Proc. IEEE Int. Symp. Ind. Electron.*, 2007, pp. 578–583.

[11] L. K. Haw, M. S. A. Dahidah, and H. A. F. Almurib, "SHE_PWM cascaded multilevel inverter with adjustable DC voltage levels control for STATCOM applications," *IEEE Trans. Power Electron.,* vol. 29, no. 12, pp. 6433–6444, Dec. 2014.

[12] C. Buccella, C. Cecati, and M. G. Cimoroni, "Performance analysis and simulation of unbalanced DC sources five level inverter topology," in *Proc. 4th Int. Conf. Renewable Energy Res. Appl.*, Palermo, Italy, Nov. 2015, pp. 1152–1156.
[13] M. Najjar, A. Moeini, M. K. Bakhshizadeh, F. Blaabjerg, and S. Farhangi, "Optimal selective harmonic mitigation technique on variable DC link cascaded H-bridge converter to meet power quality standards," *IEEE J. Emerg. Sel. Topics Power Electron.*, vol. 4, no. 3, pp. 1107–1116, Sep. 2016.
[14] M. Sharifzadeh, H. Vahedi, C. Cecati, C. Buccella, and K. Al-Haddad, "A generalized formulation of SHM-PAM for cascaded H-bridge inverters with non-equal DC sources," in *Proc. IEEE Int. Conf. Ind. Technol.*, Toronto, ON, Canada, Mar. 2017, pp. 18–23.
[15] Z. Yuan, R. Yuan, W. Yu, J. Yuan, and J. Wang, "A Groebner bases theory-based method for selective harmonic elimination," *IEEE Trans. Power Electron.*, vol. 30, no. 12, pp. 6581–6592, Dec. 2015.
[16] K. Yang, Q. Zhang, R. Yuan, W. Yu, J. Yuan, and J. Wang, "Selective harmonic elimination with Groebner bases and symmetric polynomials," *IEEE Trans. Power Electron.* vol. 31, no. 4, pp. 2742–2752, Apr. 2016.
[17] C. Buccella, C. Cecati, M. G. Cimoroni, and K. Razi, "Analytical method for pattern generation in five-level cascaded H-bridge inverter using selective harmonic elimination," *IEEE Trans. Ind. Electron.*, vol. 61, no. 11, pp. 5811–5819, Nov. 2014.
[18] C. Buccella, C. Cecati, M. G. Cimoroni, G. Kulothungan, A. Edpuganti, and A. K. Rathore, "A selective harmonic elimination method for five-level converters for distributed generation," *IEEE J. Emerg. Sel. Topics Power Electron.*, vol. 5, no. 2, pp. 775–783, Jun. 2017.
[19] C. Buccella, M. G. Cimoroni, H. Latafat, G. Graditi, and R. Yang, "Selective harmonic elimination in a seven level cascaded multilevel inverter based on graphical analysis," in *Proc. IEEE Int. Conf. Ind. Electron.*, Florence, Italy, Oct. 2016, pp. 2563–2568.
[20] S. S. Lee, B. Chu, N. R. N. Idris, H. H. Goh, and Y. E. Heng, "Switched-battery boost-multilevel inverter with GA optimized SHEPWM for standalone application," *IEEE Trans. Ind. Electron.*, vol. 63, no. 4, pp. 2133–2142, Apr. 2016.
[21] E. Suli and D. F. Mayers, *An Introduction to Numerical Analysis*, 1st ed. Cambridge, U.K.: Cambridge Univ. Press, 2003.
[22] 2018. [Online]. Available: https://www.digipower.it
[23] "DE10-Nano board," Terasic, Inc., Hsinchu, Taiwan. 2018. [Online]. Available: http://www.terasic.com.tw/cgi-bin/page/archive.pl?Language=English&CategoryNo=165&No=1046
[24] "Quartus Prime version 16.1.0," Intel, Santa Clara, CA, USA. 2018. [Online]. Available: https://www.altera.com/products/design-software/fpga-design/quartus-prime/overview.html

Concettina Buccella (M' 92–SM'03) received the M.S. degree from the University of L'Aquila, L'Aquila, Italy, in 1988, and the Ph.D. degree in electrical engineering from the University of Rome "La Sapienza," in 1995.

From 1988 to 1989, she was a Research Engineer with Italtel SpA, L'Aquila, Italy. In 1991, she joined the Department of Electrical Engineering, University of L' 'Aquila, where she has been an Associate Professor in electrotechnics since 2001. She holds three Italian Habilitations as a Full Professor in power converters, drivers, machines and power systems and in electrotechnics. Her research interests deal with smart grids, power converters modulation techniques, renewable energy management, analytical and numerical modeling.

Prof. Buccella was a corecipient of the 2012 and the 2013 Best Paper Award of the IEEE TRANSACTIONS ON INDUSTRIAL INFORMATICS. She is an Associate Editor for the IEEE TRANSACTIONS ON INDUSTRIAL ELECTRONICS, moreover, she has been the Chair of the IEEE-IES Renewable Energy Systems Technical Committee, from 2017 to 2018. She is the Chief Scientific Officer with DigiPower srl, L'Aquila, Italy, an R&D company active in the field of power electronics.

Maria Gabriella Cimoroni received the M.Sc. (*summa cum laude*) degree in mathematics from the University of L'Aquila, L'Aquila, Italy, in 1989.

After graduation, she attended the post-graduate Inter-University School, Perugia and the CNR Computational Mathematics School, Naples. Since 1994, she has been a Researcher in numerical analysis with the University of L'Aquila. Her research activities deal with new spline operators for approximation of functions, for numerical evaluation of Cauchy principal value integrals and for numerical solution of integro-differential equations and since some years with analytical and numerical methods for modulation algorithms for multilevel converters.

Prof. Cimoroni has been a reviewer for several international conferences and IEEE Transactions. She was a Publication Chair of IEEE-IECON 2016 and the Publicity Chair of 5th International Symposium on Environment Friendly Energies and Application 2018 in Rome.

Mario Tinari received the B.S. degree in industrial engineering and the M.S. degree in electrical engineering (with honors) from the University of L'Aquila, L'Aquila, Italy, in 2014 and 2016, respectively. He is currently working toward the Ph.D. degree in information engineering, computer science and mathematics at the University of L'Aquila.

He is also a Consultant with DigiPower srl, L'Aquila, Italy, an R&D company active in the field of power electronics. His current research interests includes modeling and design of power electronics circuits, efficient power conversion, renewable electrical energy systems, and smart grids.

Carlo Cecati (M' 90–SM'03–F'06) received the Dr.Ing. Degree in electrotechnical engineering from the University of L'Aquila, L'Aquila, Italy, in 1983.

Since then, he has been with the University of L'Aquila, where he is currently a Professor in industrial electronics and drives. From 2015 to 2017, he has been a Qianren Talents Professor (1000 Talents Program Distinguished Professor) with the Harbin Institute of Technology, Harbin, China. His research interests include power electronics, distributed generation, and smart grids.

Prof. Cecati was the Editor-in-Chief for the IEEE TRANSACTIONS ON INDUSTRIAL ELECTRONICS, from 2013 to 2015. He was a corecipient of the 2012 and the 2013 Best Paper Award from the IEEE Transactions on Industrial Informatics and of the 2012 Best Paper Award from the IEEE Industrial Electronics Magazine. In 2017, he was the recipient of Antony J. Hornfeck Award from the IEEE Industrial Electronics Society. He is the Chief Technical Officer at DigiPower srl, L'Aquila, Italy, an R&D company active in the field of power electronics.